

Metamodel simulation for designing monopole telecommunication antenna support structures

Johnny Homero Sánchez-Guerrero, Christian David Lagos-Zamora, Francisco Agustín Peña-Jordán & Cesar Hernán Arroba-Arroba

Facultad de Ingeniería Civil y Mecánica, Universidad Técnica de Ambato, Ecuador, jsanchez6913@uta.edu.ec, clagos6629@uta.edu.ec, fa.pena@uta.edu.ec, ch.arroba@uta.edu.ec

Received: July 26th, 2022. Received in revised form: January 31th, 2023. Accepted: February 28th, 2023.

Abstract

Finite element analysis is used to estimate the displacements and forces present in each element of a structure. This type of analysis is time consuming in pre-processing, processing, and post-processing. It also incurs considerable computational costs. A simplified methodology is therefore required to reduce design time considerably. The research involved the development and application of an experimental methodology and a simulation, using Ansys Research software's LS-DYNA module, in which loads are applied in accordance with the ANSI/TIA 222-G standard used in the telecommunications industry. The matrix method was applied, obtaining results for nodal displacement that were compared with the results of physical tests and a metamodel, showing a variation range of 8.44%. In addition, it was shown that a metamodel can be used during the pre-design stage, significantly reducing the time required for analysis.

Keywords: monopole structure; metamodel; flange connection; section inertia; direct matrix.

Simulación del metamodelo para el diseño de estructuras soporte de antenas de telecomunicaciones tipo monopolo

Resumen

El análisis por el método de los elementos finitos se utiliza para estimar los desplazamientos y fuerzas presentes en cada elemento de una estructura. Este tipo de análisis requiere mucho tiempo de preprocesado, procesado y postprocesado, implicando además un gasto computacional considerable. Siendo necesaria una metodología simplificada que reduzca considerablemente el tiempo de diseño. La investigación se desarrolló aplicando una metodología experimental y simulación en el módulo LS-DYNA del software Ansys Research, donde las cargas son aplicadas de acuerdo a la norma ANSI/TIA 222-G utilizada en la industria de las telecomunicaciones. Se aplicó el método matricial, obteniendo los resultados de desplazamientos nodales que fueron comparados con los resultados de la prueba física y los resultados del metamodelo, mostrando un rango de variación de 8.44%, además el metamodelo puede ser utilizado en la etapa de prediseño, reduciendo significativamente el tiempo de análisis.

Palabras clave: estructura de monopolo; metamodelo; conexión de brida; inercia de la sección; matriz directa.

1 Introduction

There has been an exponential increase in the use of mobile telephony in recent years, bringing with it large capital investments in the installation of structures to support communications equipment, with optimum characteristics

both in terms of design and assembly [1-6]. The typology of these structures includes self-supporting and guyed towers and tubular monopoles [7]. Tubular monopoles require less space and are also versatile in their assembly, characteristics that favor the environment and the economy alike [8]. Tubular monopoles are assembled in sections that are joined

How to cite: Sánchez-Guerrero, J.H., Lagos-Zamora, C.D., Peña-Jordán, F.A. and Arroba-Arroba, C.H., Metamodel simulation for designing monopole telecommunication antenna support structures. DYNA, 90(225), pp. 140-146, January - March, 2023.

using mechanical techniques [9]. The discontinuous nature of the sections and the mechanical contact between them introduce structural uncertainties, rendering them vulnerable to high wind loads [10-12].

The steel construction industry uses bolted assemblies, consisting of mechanical connections, steel plates and high-strength bolts, because of their high-performance and reliable clamping properties [13,14]. The best-known connections for tubular sections are the flange-type and friction-type, the latter being less sensitive to the imperfections that may be found in the plates [15-17]. Calculations and assumptions are required for the analysis of these connections because of the uncertainty associated with environmental factors and the limited availability of models. Taken together, these two factors mean that a true representation of structural responses is not available [18,19]. Ductile failure mode is determined using analytical design methods. However, experimental results suggest that brittle failure is the most common problem [20]. Finite element analysis and destructive testing allow the behavior of bolted flange-type connections to be determined [21,22].

Comparisons between experimental results and those derived from finite element analysis have given satisfactory results in determining the demand for safety and economy in flange-type connections that are subject to pure bending. Studies of flange-type joints under axial load have been useful for studies of bending capacity but are limited in number, confining the availability of general information on the design of good connections [23]. Therefore, research should be conducted using finite element analysis and design methodologies are need to be developed for flange-type connections [24].

One of the methodologies used in the literature is the metamodel (or surrogate) approach, which consists in approximating the response of the finite element analysis using analytical functions that associate input variables with results [25,26]. Optimized methodologies that have been developed for designing steel beam-column, semi-rigid connections and bolt-tightening sequences have performed extremely well in operation [27,28]. An advantage of the metamodel approach is that it reduces the computational cost that complexity represents in the process of design steel structures, which involves a lot of input data. Consequently, metamodeling is important in speeding up both analysis and design [29,30].

This research seeks to develop an optimized methodology for the design of monopole-type telecommunications towers. It uses a parametric metamodel to estimate displacements and stress in monopole sections and flange-type bolted connections. Experimental tests were carried out and simulations in Ansys LS-DYNA Research software employed.

2 Methodology

2.1 Materials

The bending test executed on the prototype structure used ASTM A36 and ASTM A500 steel for the structural sections and ASTM A325 bolts for the connections. The mechanical properties are shown in Table 1.

Table 1.
Characteristics of the material models used in Ansys Research.

| Material | Density [kg/m ³] | Young's Modulus [MPa] | Poisson's ratio | Yield Limit [MPa] | Maximum Tensile Strength [MPa] | Failure Plastic Deformation |
|--------------|------------------------------|-----------------------|-----------------|-------------------|--------------------------------|-----------------------------|
| A500 | 7890 | 200000 | 0.3 | 320 | 430 | 0.370 |
| A36 | 7890 | 200000 | 0.3 | 250 | 400 | 0.283 |
| A325 (Bolts) | 7890 | 200000 | 0.3 | 586 | 827 | |

Source: the authors

2.2 Equipment

Thickness gauges, a load cell with a capacity of 500 kg, a comparator clock and a torque meter.

2.3 Methods

For the analysis, the functional characteristics of the flange-type bolted connections were investigated and a 3D model made using Ansys SpaceClaim software. The results obtained using the finite element analysis served to parameterize the metamodel. The experimental results of the physical test supported the results of the finite elements analysis of the simulation carried out using using Ansys Research software.

The estimation of loads applied to the structure by finite elements was analyzed according to the ANSI/TIA EIA 222 – G standard, and to data on permanent loads such as the weight of the structure itself and of the accessories and communication equipment. To determine loads produced by the wind, the following data were used: wind speed 90 km/h, topographic category 2, exposure category type B. The load was at different points applied at 6 meter intervals along the 36 meter octagonal section tubular monopole. The structure is described in Table 2. For the joints between sections, a "beam" type element was used, which simulates the presence of the bolts used to join the flanges. The contact between each section's flanges was "frictionless".

The results obtained for the full-scale structure were used to estimate an equivalent prototype on a reduced scale. This was analyzed using the same software and applying the same conditions as the real structure. It was possible to visualize the deformation trend by measuring deformations at strategic points along the prototype made. To verify the behavior estimated by analysis, a real test was carried out on the prototype. A test bench was assembled, and displacement measurements were made at the top of the prototype, at different levels of force. Fig. 1 shows the results of the prototype test.

With the results of the analysis and the phase test, a simplified model was proposed (focused on areas where there was a change of section, contact between components or border conditions were present). The metamodel had two principal aims: to reproduce displacements caused by the load, which causes horizontal deformation of the structure and structural rotation with respect to its supporting plane. The simplified structure was of the two-dimensional "frame" type, with material properties, section, and length. Strategic points, where contact occurred, there was a change of section or border conditions were present were also specified.

Table 2.
Elements included in the 36-meter monopole construction.

| Section | Height [m] | Flanges | | | Tubular sections | |
|---------|------------|-----------------------|---------------|---------|------------------|----------------|
| | | Flange thickness [mm] | Diameter [mm] | # Bolts | Face width [mm] | Thickness [mm] |
| 1 | 36 | - | - | - | 230 | 6 |
| | 30 | 15 | 750 | 16 | | |
| 2 | 24 | 15 | 750 | 16 | 230 | 8 |
| | 18 | 20 | 850 | | | |
| 3 | 12 | 20 | 850 | 16 | 268 | 8 |
| | 6 | 20 | 950 | | | |
| 4 | 12 | 20 | 950 | 16 | 306 | 10 |
| | 6 | 25 | 1050 | | | |
| 5 | 6 | 25 | 1050 | 16 | 345 | 10 |
| | 0 | 25 | 1150 | | | |
| 6 | 0 | 38 | 1150 | 24 | 383 | 12 |

Source: the authors

The simplified model is shown by the light blue line in Fig. 2 and the equivalent strut load allowed the visualization of a reduced scheme that facilitated the analysis of the data obtained using finite element analysis. These were obtained for the points where a section change was present that define the behavior of the structure, because of the important deformations that occur, in particular in the flanged connections.

The prototype was assembled using tubular sections of 101 mm (4 in.) diameter with 4 mm (3/16 in.) thickness; the flanges were 175 mm (6 7/8 in.) in diameter and 10 mm (3/8 in.) thick; the gussets were triangular, with a 35 mm (1 3/8 in.) base, 101 mm (4 in.) height and 6 mm (1/4 in.) thickness in the upper section and 8 mm (5/16 in.) in the lower section. The prototype was 2 meters tall. Fig. 2 shows the elements and nodes used. Each node had 3 degrees of freedom: displacement in the X axis (δX_i), displacement in the Y axis (δY_i) and rotation in the Z axis (θ_i), with force applied at node 12 ($F=2533.4$ N). Each element had its equivalent stiffness (k_i), with the result that the equilibrium could be described using eq. (1):

$$[F]=[k_i]*[\delta] \tag{1}$$

$$[k_i]=\frac{EI}{L_i} \begin{bmatrix} A_i C_i^2 + \frac{12I_i}{L_i^2} S_i^2 & \left(A_i - \frac{12I_i}{L_i^2}\right) C_i S_i & -\frac{6I_i}{L_i} S_i & -\left(A_i C_i^2 + \frac{12I_i}{L_i^2} S_i^2\right) & -\left(A_i - \frac{12I_i}{L_i^2}\right) C_i S_i & -\frac{6I_i}{L_i} S_i \\ \left(A_i - \frac{12I_i}{L_i^2}\right) C_i S_i & A_i S_i^2 + \frac{12I_i}{L_i^2} C_i^2 & \frac{6I_i}{L_i} C_i & -\left(A_i - \frac{12I_i}{L_i^2}\right) C_i S_i & -\left(A_i S_i^2 + \frac{12I_i}{L_i^2} C_i^2\right) & \frac{6I_i}{L_i} C_i \\ -\frac{6I_i}{L_i} S_i & \frac{6I_i}{L_i} C_i & 4I_i & \frac{6I_i}{L_i} S_i & -\frac{6I_i}{L_i} C_i & 2I_i \\ -\left(A_i C_i^2 + \frac{12I_i}{L_i^2} S_i^2\right) & -\left(A_i - \frac{12I_i}{L_i^2}\right) C_i S_i & \frac{6I_i}{L_i} S_i & A_i C_i^2 + \frac{12I_i}{L_i^2} S_i^2 & \left(A_i - \frac{12I_i}{L_i^2}\right) C_i S_i & \frac{6I_i}{L_i} S_i \\ -\left(A_i - \frac{12I_i}{L_i^2}\right) C_i S_i & -\left(A_i S_i^2 + \frac{12I_i}{L_i^2} C_i^2\right) & -\frac{6I_i}{L_i} C_i & \left(A_i - \frac{12I_i}{L_i^2}\right) C_i S_i & A_i S_i^2 + \frac{12I_i}{L_i^2} C_i^2 & -\frac{6I_i}{L_i} C_i \\ -\frac{6I_i}{L_i} S_i & \frac{6I_i}{L_i} C_i & 2I_i & \frac{6I_i}{L_i} S_i & -\frac{6I_i}{L_i} C_i & 4I_i \end{bmatrix}$$

Where:

- A_i = Equivalent area of the element.
- I_i = Inertia of the element
- L_i = Length of the element
- E_i = Modulus of elasticity of the element
- S_i = Sine of the angle of element orientation
- C_i = Cosine of the angle of element orientation

Elements 2, 10 and 12 are the joints between sections. These displayed a non-linear behavior. For this reason, the metamodel was required to considers this reinforced section, calculating an equivalent length that represented the physical properties of the reinforced section, using eq. (2):

$$L_{equ} = \sqrt[4]{12 * I_b} \tag{2}$$

Where:

- L_{equ} = Equivalent length
- I_b = Inertia of the reinforced assembly: flanges, bolts, gussets.

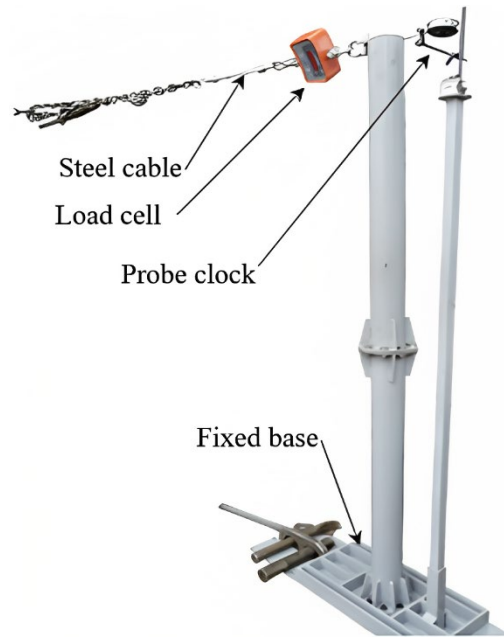


Figure 1. Prototype of the monopole structure on the test bench.
Source: the authors

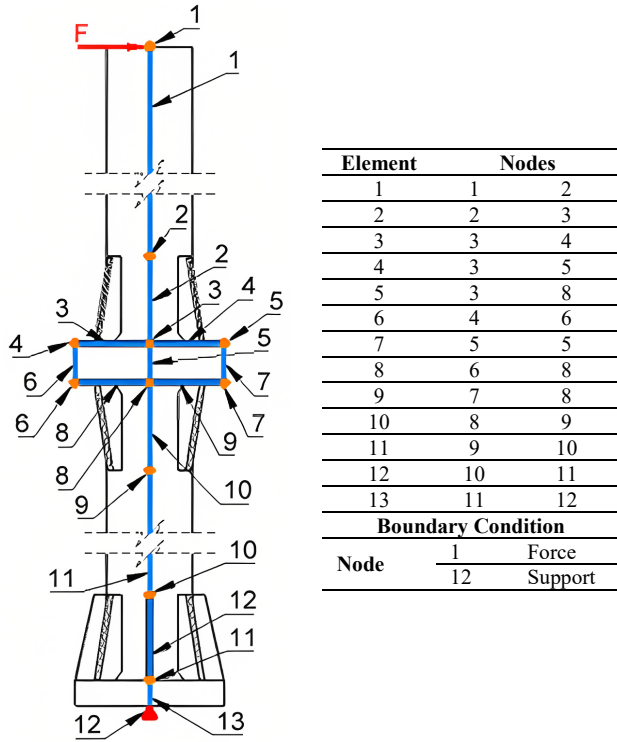


Figure 2. Identification of elements and nodes, from the prototype in Fig. 1. Source: the authors

1 Results

According to the finite element analysis the displacement of the 36000 mm structure was about 400 mm, resulting in a rotation angle of 1/90. The angle of rotation was equal at all heights, allowing an equivalent deformation for the prototype to be calculated:

$$\delta p = \frac{1}{90} 2000mm = 22.22 mm$$

In addition to the figures for displacement, a stress of 300 MPa was obtained, located in section 3 at a height of 18 meters. Data for the prototype was obtained using the description provided in Fig. 2. Fig. 3 shows the stress and displacement results both for the 36-meter structures and the prototype.

Table 3 shows the results obtained by physical testing, finite element analysis and the data estimated using the metamodel. Note that the data for the three types of analysis are very approximate.

Fig. 4 shows the comparative graph of the data presented in Table 2, showing that the three types of analysis follow the same trend.

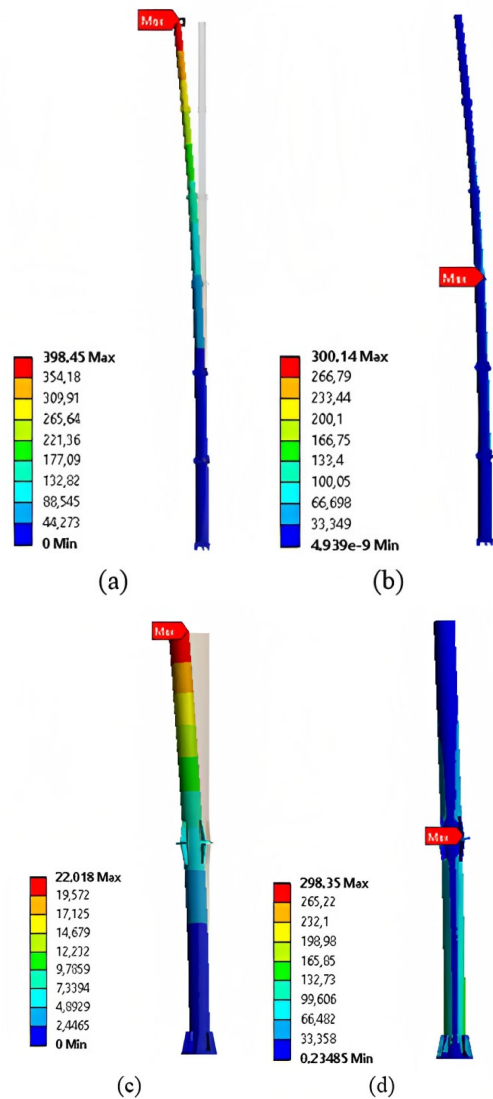


Figure 3. Finite element analysis results. (a) Displacement of the 36-meter monopole, (b) Maximum stress of the 36-meter monopole located at 50% height, (c) Displacement of the monopole prototype, (d) Maximum stress of the monopole prototype located at 50% height. Source: the authors

Table 3. Results of physical testing, finite element analysis and metamodel.

| Force [N] | Z-axis displacement [mm] | | |
|-----------|--------------------------|-----------|-----------|
| | Physical Test | FEM Solid | Metamodel |
| 196.2 | 1.6520 | 1.7053 | 1.7422 |
| 392.4 | 3.2300 | 3.4105 | 3.4844 |
| 588.6 | 4.9533 | 5.1158 | 5.2266 |
| 784.8 | 6.5500 | 6.8210 | 6.9688 |
| 981.0 | 8.3067 | 8.5263 | 8.7110 |
| 1177.2 | 10.0733 | 10.2320 | 10.4532 |
| 1373.4 | 12.1800 | 11.9370 | 12.1954 |
| 1569.6 | 13.6500 | 13.6420 | 13.9376 |
| 1765.8 | 15.5667 | 15.3470 | 15.6798 |
| 1962.0 | 17.1217 | 17.0530 | 17.4220 |
| 2158.2 | 19.1233 | 18.7580 | 19.1643 |
| 2354.4 | 20.9300 | 20.0190 | 20.9075 |
| 2533.4 | 22.5900 | 22.0190 | 22.4959 |
| 2550.6 | 22.7467 | 22.1630 | 22.6487 |

Source: the authors

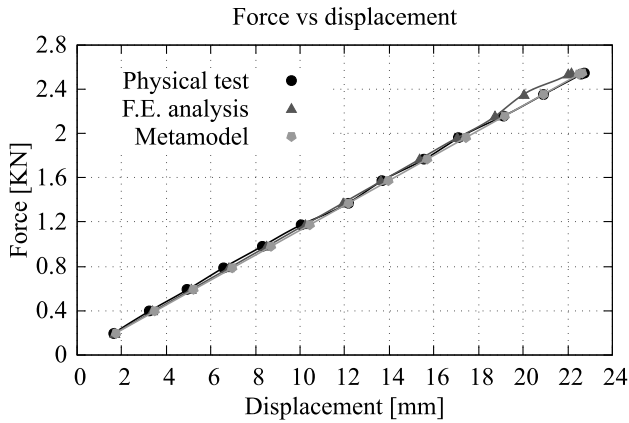


Figure 4. Comparison of results for the prototype, obtained by the physical test, finite element analysis and metamodel.
Source: the authors

Table 4. Results of the displacements of the 36-meter monopole and its respective metamodel.

| Height [m] | Z-axis displacement [mm] | | |
|------------|--------------------------|-----------|---------------|
| | FEM Solid | Metamodel | Variation [%] |
| 36 | 398.45 | 425.60 | 6.38 |
| 30 | 268.63 | 290.32 | 7.47 |
| 24 | 159.96 | 173.43 | 7.77 |
| 18 | 82.65 | 90.27 | 8.44 |
| 12 | 34.28 | 37.42 | 8.39 |
| 6 | 7.89 | 8.58 | 8.04 |
| 0 | 0.02 | 0 | 0.00 |

Source: the authors

Table 4 shows the results of displacements of the 36-meter monopole at different heights and their respective metamodel. The maximum variation between results were 8.44%.

Fig. 5 shows the comparative graph of the results presented in Table 3. The results obtained in the prototype test validate the three-dimensional model of the analysis of the 36-meter structure. That is, the results of the analysis are reliable and may be used to compare the data calculated using the metamodel.

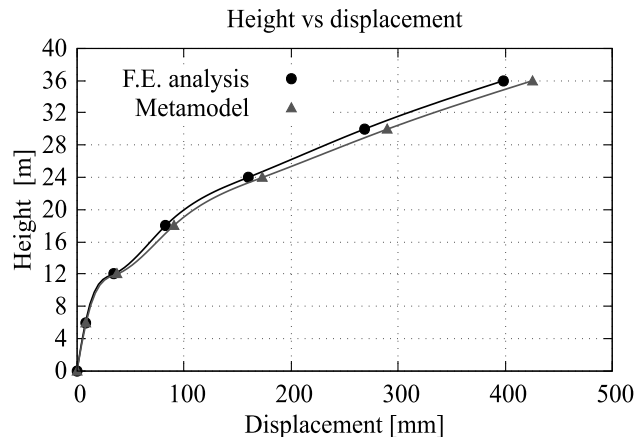


Figure 5. Comparison of results obtained in the finite element and the metamodel analysis of the 36-meter monopole.
Source: the authors

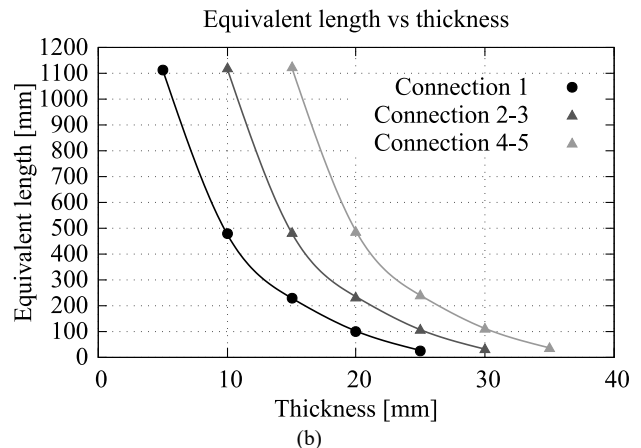
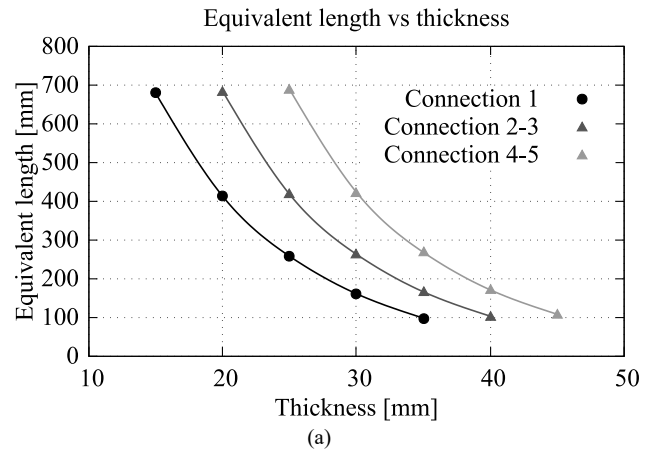
Table 5. Equivalent lengths for different combinations of flange thickness and numbers of bolts.

| Joint | 6 m (Connection 1) | | 12 m -18 m (Connection 2-3) | | 24 m - 30 m (Connection 3-4) | |
|-------|--------------------|------------------|-----------------------------|------------------|------------------------------|------------------|
| | Thickness | Equ. length [mm] | Thickness | Equ. length [mm] | Thickness | Equ. length [mm] |
| 8 | 35 | 98 | 40 | 103 | 45 | 108 |
| | 30 | 161 | 35 | 166 | 40 | 171 |
| | 25 | 258 | 30 | 263 | 35 | 268 |
| | 20 | 413 | 25 | 418 | 30 | 423 |
| | 15 | 679 | 20 | 684 | 25 | 689 |
| 16 | 25 | 26 | 30 | 31 | 35 | 36 |
| | 20 | 101 | 25 | 106 | 30 | 111 |
| | 15 | 229 | 20 | 234 | 25 | 239 |
| | 10 | 477 | 15 | 482 | 20 | 487 |
| | 5 | 1114 | 10 | 1119 | 15 | 1124 |
| 24 | 15 | 55 | 20 | 60 | 25 | 65 |
| | 10 | 191 | 15 | 196 | 10 | 201 |
| | 5 | 461 | 10 | 466 | 15 | 471 |

Source: the authors

The metamodel considered the stiffness effects caused by bolted joints, for which an equivalent length with its respective stiffness was established. The results are shown in Table 5.

Fig. 6 shows the comparative plots of data from Table 4, showing the dependence of thickness on effective length.



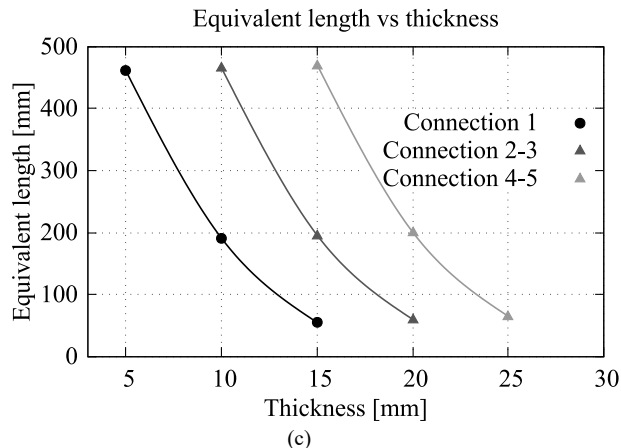


Figure 6. Comparison of equivalent length results for different combinations of flange thickness and number of bolts: (a) 8 bolts, (b) 16 bolts, (c) 24 bolts. Source: the authors

2 Conclusions

The physical test permitted the accurate determination of the contacts between "frictionless" flanges, and the representation of the bolts with "beam" type element, which were applied using the Ansys Research software and reproduced results in accordance with reality.

When compared with the results of the physical test, the results for displacement and maximum stresses obtained using the finite element analysis validated the methodology used in the metamodel approach.

The number of bolts had a direct influence on the thickness of the flanges; it is also evident that the structure's joint compartments followed a decreasing exponential trend.

References

- [1] Kumar, P., Raju, M., Navya, M., et al., Effect of wind speed on structural behaviour of Monopole and self-support telecommunication towers, *Asian Journal of Civil Engineering*, 18(6), PP. 911-927, 2017.
- [2] Kaveh, A., and Kaveh, A., Optimal design of the monopole structures using the CBO and ECBO algorithms, *Applications of Metaheuristic Optimization Algorithms in Civil Engineering*, Springer International Publishing, USA, 2017, pp. 185-199
- [3] Suryakumar, V.S., Liu, Z., et al., Aeroelastic preliminary-design optimization of communication tower structures, *AIAA Scitech 2020 Forum*, 2020, pp. 1-15. DOI: <https://doi.org/10.2514/6.2020-1634>
- [4] Gao, S. and Wang, S., Progressive collapse analysis of latticed telecommunication towers under wind loads, *Advances in Civil Engineering*, 2018, art. 3293506, 2018. DOI: <https://doi.org/10.1155/2018/3293506>
- [5] Ahmad, S.I., Alam, M.S., and Alam, M.J., Structural and life-cycle economic feasibility of rooftop low-height bamboo telecom tower considering a case study from bangladesh, *Practice Periodical on Structural Design and Construction*, 25(3), art. 492, 2020. DOI: [https://doi.org/10.1061/\(asce\)sc.1943-5576.0000492](https://doi.org/10.1061/(asce)sc.1943-5576.0000492)
- [6] Szafran, J., Juszczak-Andraszyk, K., and Kamiński, M., Reinforcements of tower structures: effective and economic design engineering, in: *Proceedings of XXIV LSCE Conference 2018*, Łódź University of Technology, 2018, pp.126-133.
- [7] Travanca, R., Varum, H., and Vila-Real, P., The past 20 years of telecommunication structures in Portugal, *Engineering Structures*, 48, pp. 472-485, 2013. DOI: <https://doi.org/10.1016/j.engstruct.2012.10.012>
- [8] Al-jassani, A., and Al-suraifi, I., Telecommunication cell tower most common alternatives, *American Journal of Civil Engineering*, 5(5), pp. 268-281, 2017. DOI: <https://doi.org/10.11648/j.ajce.20170505.12>
- [9] Varghese, J. and Joseph, R., Analysis of monopole communication tower, *International Journal of Engineering Studies and Technical Approach*, 2015, pp. 23-34
- [10] Giaccu, G.F., Modeling a gyroscopic stabilizer for the improvement of the dynamic performances of slender monopole towers, *Engineering Structures*, 215, art. 110607, 2020. DOI: <https://doi.org/10.1016/j.engstruct.2020.110607>
- [11] Luan, Y., Guan, Z., Cheng, G., et al., A simplified nonlinear dynamic model for the analysis of pipe structures with bolted flange joints, *Journal of Sound and Vibration*, 331(2), pp. 325-344, 2020. DOI: <https://doi.org/10.1016/j.jsv.2011.09.002>
- [12] Giaccu, G.F. and Caracoglia, L., Wind-load fragility analysis of monopole towers by Layered Stochastic-Approximation-Monte-Carlo method, *Engineering Structures*, 174, pp. 462-477, 2018. DOI: <https://doi.org/10.1016/j.engstruct.2018.07.081>
- [13] Yu, Q., Zhou, H., et al., High-temperature low cycle fatigue life prediction and experimental research of pre-tightened bolts, *Metals*, 8(10), art. 828, 2018. DOI: <https://doi.org/10.3390/met8100828>
- [14] Badara-Camara, A., Pennec, F., et al., Fatigue life assessment of bolted connections, *MATEC Web of Conferences*, 12th International Fatigue Congress (FATIGUE 2018), 165, art. 10009, 2018. DOI: <https://doi.org/10.1051/mateconf/201816510009>
- [15] Pavlović, M., Heistermann, C., Veljković, M., et al., Friction connection vs. Ring flange connection in steel towers for wind converters, *Engineering Structures*, 98, pp. 151-162, 2015. DOI: <https://doi.org/10.1016/j.engstruct.2015.04.026>
- [16] Huang, F., Zhang, D., Hong, W., and Li, B., Mechanism and calculation theory of prying force for flexible flange connection, *Journal of Constructional Steel Research*, 132, pp. 97-107, 2017. DOI: <https://doi.org/10.1016/j.jcsr.2017.01.014>
- [17] Deng, H., Song, X., et al., Experiment and design methodology of a double-layered flange connection in axial loads, *Engineering Structures*, 175, pp. 436-456, 2018. DOI: <https://doi.org/10.1016/j.engstruct.2018.08.040>
- [18] Meisami, F. and Moavenian, M., Nonlinear behavior of single bolted flange joints: a novel analytical model non-linear modeling and dynamic analysis of bolted flange joints view project, *Engineering Structures*, 173, pp. 908-917, 2018. DOI: <https://doi.org/10.1016/j.engstruct.2018.07.035>
- [19] Tessari, R.K., Kroetz, H.M., and Beck, A.T., Performance-based design of steel towers subject to wind action, *Engineering Structures*, 143, pp. 549-557, 2017. DOI: <https://doi.org/10.1016/j.engstruct.2017.03.053>
- [20] Van-Long, H., Jean-Pierre, J., and Jean-François, D., Behaviour of bolted flange joints in tubular structures under monotonic, repeated and fatigue loadings I: experimental tests, *Journal of Constructional Steel Research*, 85, pp. 1-11, 2013. DOI: <https://doi.org/10.1016/j.jcsr.2013.02.011>
- [21] Blachowski, B., Gutkowski, W., Effect of damaged circular flange-bolted connections on behaviour of tall towers, modelled by multilevel substructuring, *Engineering Structures*, 111, pp. 93-103, 2016. DOI: <https://doi.org/10.1016/j.engstruct.2015.12.018>
- [22] Szafran, J. and Rykaluk, K., A full-scale experiment of a lattice telecommunication tower under breaking load, *Journal of Constructional Steel Research*, 120, pp. 160-175, 2016, DOI: <https://doi.org/10.1016/j.jcsr.2016.01.006>
- [23] Wang, Y., Zong, L., and Shi, Y.J., Bending behavior and design model of bolted flange-plate connection, *Journal of Constructional Steel Research*, 84, pp. 1-16, 2013. DOI: <https://doi.org/10.1016/j.jcsr.2013.01.012>
- [24] Hawkins, D.W., Discussion of current issues related to steel telecommunications monopole structures, in: *Structures Congress 2010*, 2010, pp. 2417-2438. DOI: [https://doi.org/10.1061/41130\(369\)219](https://doi.org/10.1061/41130(369)219)
- [25] Fernandez-Ceniceros, J., Sanz-García, A., et al., A numerical-informational approach for characterising the ductile behaviour of the T-stub component. Part 2: parsimonious soft-computing-based metamodel, *Engineering Structures*, 82, pp. 249-260, 2015. DOI: <https://doi.org/10.1016/j.engstruct.2014.06.047>

- [26] Loureiro, A., Lopez, M., et al. Metamodelling of stiffness matrices for 2D welded asymmetric steel joints, *Journal of Constructional Steel Research*, 162, art. 105703, 2019. DOI: <https://doi.org/10.1016/j.jcsr.2019.105703>
- [27] Díaz, C., Victoria, M., et al., Optimum design of semi-rigid connections using metamodells, *Journal of Constructional Steel Research*, 78, pp. 97-106, 2012. DOI: <https://doi.org/10.1016/j.jcsr.2012.06.013>
- [28] Abasolo, M., Aguirrebeitia, J., et al., Methodology for the optimization of bolting sequences for wind generator flanges, *Journal of Pressure Vessel Technology*, ASME, 136(6), art. 061202, 2014. DOI: <https://doi.org/10.1115/1.4027597>
- [29] Arroba, C.H., Penã, F.A., et al., Simulating metamodel for urban bus seats design, *IOP Conference Series: Materials Science and Engineering*, 507(1), Incheon, South Korea, 2019, art. 012027. DOI: <https://doi.org/10.1088/1757-899X/507/1/012027>
- [30] Wan, H.P. and Ren, W.X., Parameter selection in finite-element-model updating by global sensitivity analysis using gaussian process metamodel, *Journal of Structural Engineering*, 141(6), art. 1108, 2015. DOI: [https://doi.org/10.1061/\(ASCE\)ST.1943-541X.0001108](https://doi.org/10.1061/(ASCE)ST.1943-541X.0001108).

J.H. Sanchez-Guerrero is BSc. Eng. in Mechanical Engineer in 2019, from the *Universidad Técnica de Ambato*, Ambato, Ecuador. In 2020 he obtained certification as a Mechanical Designer. From 2019 he worked in mechanical engineering programs and projects, with an emphasis on mechanical design and simulation, collaborating with the *Universidad Técnica de Ambato* in the publication of articles in scientific journals. He works in the design, detailing and assembly of metal structures.
ORCID: 0000-0002-3119-7139

C.D. Lagos-Zamora is BSc. Eng. in Mechanical Engineer in 2019, from the *Universidad Técnica de Ambato*, Ambato, Ecuador. From 2019 he worked in mechanical engineering programs and projects, with emphasis on mechanical design and simulation, collaborating with the *Universidad Técnica de Ambato* in the publication of articles in scientific journals. He works in the design, detailing and assembly of metal structures.
ORCID: 0000-0003-2488-9265

F.A. Peña-Jordán is BSc. Eng. in Mechanical Engineer in 2007, from the *Universidad Técnica de Ambato*, Ambato, Ecuador and obtained an MSc. in Mechanical Design in 2016, from the *Escuela Politécnica Nacional*, Quito, Ecuador and a MSc. in Civil Engineering in 2022, from the *Universidad Técnica de Ambato*, Ambato, Ecuador. He graduated as a Sp. in steel building design from the *Universidad CLEA* in 2023. He has worked in the design, detailing and assembly of metal structures. He is a full-time professor at the *Universidad Técnica de Ambato* in the Faculty of Civil and Mechanical Engineering. His research interests include the simulation of steel structures for the telecommunication industry, welded and bolted connections and foundations.
ORCID: 0000-0002-0140-3827

C.H. Arroba-Arroba is BSc. Eng. in Mechanical Engineer in 2003, from the Polytechnic School of Chimborazo. Riobamba, Ecuador. He obtained a MSc. in Mechanical Design in 2013, from the *Universidad Técnica de Ambato*, Ambato, Ecuador. Currently, he is a full-time professor at the *Universidad Técnica de Ambato* in the Faculty of Civil and Mechanical Engineering. Since 2013, he has researched bus design, steel structures and numerical simulation.
ORCID: /0000-0001-5656-7549